Published in final edited form as:
J Phys Chem B. 2012 June 21; 116(24): 7138–7144. doi:10.1021/jp303269m.

Utilizing Afterglow Magnetization from Cross-Polarization Magic-Angle-Spinning Solid-State NMR Spectroscopy to Obtain Simultaneous Heteronuclear Multidimensional Spectra

James R. Banigan and **Nathaniel J. Traaseth***
Department of Chemistry, New York University, New York, NY 10003

Abstract

The time required for data acquisition and subsequent spectral assignment are limiting factors for determining biomolecular structure and dynamics using solid state NMR spectroscopy. While strong magnetic dipolar couplings give rise to relatively broad spectra lines, the couplings also mediate the coherent magnetization transfer via the Hartmann Hahn cross polarization (HH-CP) experiment. This mechanism is used in nearly all backbone assignment experiments for carrying out polarization transfer between ^{1}H, ^{15}N, and ^{13}C. In this Article, we describe a general spectroscopic approach to use the residual or *afterglow* magnetization from the ^{15}N to ^{13}C selective HH-CP experiment to collect a second multidimensional heteronuclear dataset. This approach allowed for the collection of two multidimensional (2D NCA and NCO or 3D NCACX and NCOCX) datasets at the same time. These experiments were performed using instrumentation available on all standard solid state NMR spectrometers configured for magic angle spinning and were demonstrated on uniformly [^{13}C,^{15}N] and [1,3-^{13}C] glycerol labeled ubiquitin. This method is compatible with several other sensitivity enhancement experiments and can be used as an isotopic filtering tool to reduce the spectral complexity and decrease the time needed for assigning spectra.

Keywords

NMR; solid state NMR; crystals; proton driven spin diffusion; assignment methods; ubiquitin; fast data acquisition; sequential acquisition; detection approaches

Introduction

Solid-state NMR magic-angle-spinning (SSNMR MAS) is a widely used method to probe structure and dynamics of hard and soft biological matter.[1-7] One of the main bottlenecks in this process is assigning the spectra, which can be especially challenging for membrane proteins and amyloid samples. To address this problem, a number of ways have been proposed to improve the spectral resolution and sensitivity of data acquisition. These can be broadly grouped into three categories: (1) spectroscopic based (e.g., pulse sequences, data acquisition), (2) sample preparation (e.g., isotopic labeling, paramagnetic labeling), and (3) advances in instrumentation (e.g., multiple receivers, cryogenic probes). Combined spectroscopic and instrumentation approaches such as simultaneous or sequential data acquisitions have been applied to the time-consuming process of spectral assignment

*Author for correspondence: Nathaniel J. Traaseth, 100 Washington Square East, New York, NY 10003, Phone: (212) 992-9784, traaseth@nyu.edu.

Supporting Information
The pulse sequence in Figure 1 can be downloaded from our website: www.nyu.edu/fas/dept/chemistry/traasethgroup/

through the improvement of these triple resonance techniques that shorten data acquisition times.[8-11]

A novel solution NMR approach recently introduced by Kupce *et al*. utilizes the residual or "afterglow" ^{13}C magnetization for the purpose of acquiring multiple heteronuclear spectra at the same time.[9] In this pulse sequence, the ^{13}C magnetization was directly detected to acquire a 2D (HA)CACO experiment nuclease A inhibitor in the *standard* way. The residual ^{13}CO magnetization was then transferred to ^{15}N and finally detected using the sensitive $^{1}H_N$ magnetization in a 3D (HA)CA(CO)NNH experiment. Since ^{13}C and ^{1}H signals were detected, these experiments made use of parallel acquisition requiring two receivers. Unlike this solution NMR methodology that relied on J-couplings, the most important transfer mechanism in oriented and MAS SSNMR is the Hartmann Hahn cross-polarization (HH-CP).[12-15] This experiment utilizes matched spinlocks on two channels resulting in coherent polarization transfer from one nucleus to the other. Since the CP is the basic element for nearly all SSNMR applications, a tremendous amount of effort has been devoted to understanding and improving this experiment,[16-20] including the use of multiple contact pulses.[12,21] Transfer of magnetization among low frequency ^{15}N and ^{13}C most commonly utilizes the double CP[22-26] or other novel polarization transfer approaches.[27-32]

A new application of the CP experiment was recently proposed and demonstrated using RNA in SSNMR spectroscopy. This triple resonance cross polarization method uses ^{1}H to simultaneously polarize ^{13}C and ^{15}N with subsequent parallel acquisition using two receivers.[8] This scheme has been applied to obtain sequentially acquired datasets that give a ^{13}C-^{13}C correlation spectrum and a heteronuclear ^{13}C-^{15}N (NCA or NCO) correlation spectrum using a single receiver (DU-MAS).[10] Careful optimization of the simultaneous cross-polarization will give only small losses on the transfer from ^{1}H to both ^{15}N and ^{13}C as compared to the double resonance CP experiment. These methods and others listed above rely on relatively long ^{15}N and ^{13}C T_1 and $T_{1\rho}$ values in soft and hard matter, including membrane proteins in oriented lipid bilayers.[33,34]

To improve the efficiency of data acquisition in SSNMR MAS, we describe an approach to detect residual or "afterglow" magnetization resulting from the double CP experiment involving selective transfer from ^{15}N to ^{13}CA. We show that this ^{15}N magnetization is appreciable and can be used to obtain a second multidimensional heteronuclear correlation experiment with good sensitivity. In practice, the result is the detection of two 2D (NCA and NCO) or two 3D (NCACX and NCOCX) experiments at the *same time* (i.e., *two for the price of one*). These experiments do not require special instrumentation, and are therefore applicable to all spectroscopic approaches where residual coherence can be salvaged for increasing the speed of data acquisition.

Experimental Methods

Sample Preparation

Ubiquitin was expressed in BL21(DE3) *E. coli* bacteria in the presence of uniformly labeled $^{13}C_6$-glucose and ^{15}N-ammonium chloride in minimal media (M9) and purified as previously described.[35] The glycerol labeling experiment was achieved by replacing glucose with [1,3-^{13}C] glycerol (1 g/L) and natural abundance sodium carbonate (1 g/L).[36,37] For preparation of the solid-state NMR samples, 10 mg of ubiquitin was dissolved in 400 Fl 20 mM sodium citrate at pH 4.1. Crystallization was initiated by the dropwise addition of 2-methyl-2,4-pentanediol (MPD) to a final concentration of 60% and allowed to proceed overnight at 4 °C.[38] The samples were packed into 3.2 mm MAS rotors using samples spacers to prevent sample dehydration.

NMR Spectroscopy

All NMR experiments were carried out using a DDR2 Agilent NMR spectrometer operating at a ^{1}H frequency of 600 MHz. The temperature was set to 0 °C and the MAS rate was 12500 ± 5 Hz. The initial cross-polarization from ^{1}H to ^{15}N utilized a contact time of 1 msec. The transfers between ^{15}N to ^{13}CA and ^{15}N to ^{13}CO utilized SPECIFIC-CP[23], a form of double CP,[25] where the ^{15}N offset was set to 121 ppm, the ^{13}CA offset to 57.5 ppm, and the ^{13}CO offset to 175 ppm. The ^{15}N to ^{13}CA transfer used a tangent adiabatic ramp[22] on the ^{15}N channel, while the ^{13}CO SPECIFIC-CP utilized the ramp on the carbon channel. The $\Delta/2\pi$ and $\beta/2\pi$ parameters of the adiabatic cross-polarization were set to 1.2 kHz and 0.3 kHz for the ^{15}N to ^{13}CA transfer and 3.7 kHz and 0.9 kHz for the ^{15}N to ^{13}CO transfer (see Eqns. 1 and 2 of Franks *et al.*[39]) with the total length of the cross-polarization time set to 4 msec. All parameters were optimized to obtain maximal signal intensity in the standard 1D NCO and NCA experiments. Both sequential data acquisition periods used a ^{13}C spectral width of 100 kHz and an acquisition time of 20 msec. The indirect ^{15}N dimension was acquired with a spectral width of 3125 Hz and 28 increments. A total of 64 and 128 scans were used for the [U-^{13}C,^{15}N] and [1,3-^{13}C] glycerol labeled ubiquitin samples, respectively. For spin diffusion experiments between ^{13}C spins, the DARR condition was set to the n=1 rotary resonance condition on ^{1}H (12.5 kHz).[40]

Results

Sequential Acquisition of Residual ^{15}N Magnetization

The standard experiments for obtaining resonance assignments and distance restraints in MAS utilize multiple transfers between ^{15}N and ^{13}CA or ^{15}N and ^{13}CO. The NCACX and NCOCX experiments are two of the most valuable that give correlations among the backbone nuclei. The former correlates intra-residue carbon atoms with the chemical shifts of ^{15}N and ^{13}CA. This involves a HH-CP element where ^{1}H polarization is transferred to ^{15}N and followed by a ^{15}N chemical shift evolution in t_1. Magnetization is then most commonly transferred to ^{13}CA using a type of double cross polarization[25] called SPECIFIC CP.[23] After the transfer, ^{13}CA chemical shifts are evolved in the t_2 time dimension and then allowed to undergo spin diffusion most commonly with a DARR mixing period.[40] Finally, the ^{13}C magnetization is detected in the direct dimension. These are the standard experiments carried out and will be referred to as the STD-NCA or STD-NCACX (with DARR).

Following the SPECIFIC-CP transfer to ^{13}CA, there is residual ^{15}N magnetization remaining that is typically discarded. Using [U-^{15}N,^{13}C] ubiquitin, we carried out the 1D NCA experiment detecting on ^{15}N immediately following the SPECIFIC-CP transfer to ^{13}CA. Relative to the ^{15}N magnetization after CP from ^{1}H, ~40-45% of the ^{15}N signal remained. Therefore, it is possible to detect this ^{15}N polarization at the same time as the STD-NCA ^{13}C detected experiment with a second receiver (parallel acquisition[11]). However, 1D spectra do not provide the resolution required for resolving all the protein resonances. Instead, the pulse sequence in Figure 1 shows how *afterglow* (or residual) ^{15}N signal can be salvaged to obtain a second 2D NCO or 3D NCOCX dataset. The first half of the pulse sequence in Figure 1 is identical to that of a standard NCA (or NCACX) experiment. To reuse the residual ^{15}N magnetization, a 90° pulse is applied to ^{15}N spins immediately following the SPECIFIC-CP transfer to ^{13}CA. This stores the magnetization along the z-axis. Since the T_1 relaxation times for ^{15}N in proteins are on the order of seconds, placing the spins along the z-axis results in only a small amount of magnetization lost due to longitudinal relaxation. Following the free-induction-decay acquisition for the 2D NCA (or 3D NCACX) experiment, a 90_x° pulse is applied to ^{15}N placing it along the y-axis. Next, a second SPECIFIC-CP step is used to transfer magnetization to ^{13}CO in the same

way as a standard NCO experiment. The ^{13}CO magnetization is then directly detected to obtain a 2D NCO or evolved in the indirect t_2' dimension followed by a DARR mixing element to give a 3D NCOCX experiment. If evolved in the indirect dimension, t_2' is arrayed concurrently with the ^{13}CA t_2 evolution period for the NCACX experiment. Both simultaneously acquired datasets have an identical ^{15}N chemical shift evolution period (t_1). For brevity, we will refer to the sequentially acquired datasets using the following nomenclature: SIM_1-NCA or SIM_1-NCACX (first dataset acquired) or SIM_2-NCO or SIM_2-NCOCX (second dataset acquired); the standard experiments will be called STD-NCA, STD-NCO, STD-NCACX, or STD-NCOCX.

Application to Uniformly Labeled Ubiquitin

We carried out the pulse sequence in Figure 1 on selectively and uniformly labeled ubiquitin prepared in a microcrystalline state. [U-^{13}C,^{15}N] ubiquitin has 76 residues and therefore 76 ^{15}N-^{13}CA pairs. The 2D STD-NCA and SIM_1-NCA datasets on [U-^{13}C,^{15}N] ubiquitin are shown in Figure 2. These spectra give the same signal to noise, which is expected since the first half of the pulse sequence in Figure 1 is identical to the STD-NCA experiment. After the first transfer from ^{15}N to ^{13}CA, the amount of ^{15}N magnetization available for the ^{15}N to ^{13}CO SPECIFIC-CP is reduced. This results in an overall signal intensity of the SIM_2-NCO 2D dataset of 32 ± 3% compared to that of the STD-NCO. However, the SIM_2-NCO gives ~50% the signal/noise as the SIM_1-NCA, which results from the slightly better efficiency of the ^{15}N to ^{13}CO vs. ^{15}N to ^{13}CA SPECIFIC-CP experiment.[39,41] Although the second dataset is lower in intensity (see 1D cross sections in Figure 3), the SIM_2-NCO is a *free* dataset since the preparation and subsequent detection of the *afterglow* ^{15}N magnetization only adds ~25 msec to the overall pulse sequence. In practice, for a recycle delay of 2 sec and an acquisition period of 25 msec, the pulse sequence in Figure 1 only increases the experimental time by 1.2% relative to the STD-NCA. If a 3 sec recycle delay is used, this amounts to an increase of 0.8%.

There are ~45-50 resonances within the NCA spectra shown in Figure 2 out of the 76 residues in ubiquitin. It has been reported that nine peaks do not appear as a result of residual motion in the loop encompassing residues 8-10 and the C-terminus (residues 71-76) at 0 °C.[38] In addition, some of the peaks have reduced signal intensity based on crystallization with MPD or polyethylene glycol (PEG).[42] For example, in the 2D N-CA spectrum reported by Seidel *et al.* crystallized from PEG, there are four clearly resolved Gly peaks (G10, G35, G47, and G53), however, in the ubiquitin N-CA spectrum reported by Schubert *et al.* prepared by crystallization using MPD (same as the ubiquitin preparations used in this study), only G35 and G47 were observed.[43] The lack of the Gly10 peak is consistent with the cross-polarization based results from Igumenova *et al.*[38] These observations from the literature as well as our detection of an additional ~3-5 peaks at a reduced contour level from the data in Figure 2 account for the large majority of the expected resonances in ubiquitin. To identify the remaining spin systems, experiments at a higher magnetic field and/or 3D spectroscopy can be used.[44]

The 3D version of the SIM_2-NCOCX and SIM_1-NCACX datasets evolve the ^{13}CO and ^{13}CA dimensions together in t_2' and t_2, respectively. It is important to realize that the dwell times for the ^{13}CO and ^{13}CA dimensions can be different, which is beneficial since the ^{13}CA chemical shift range is ~30 ppm, while the ^{13}CO region is ~10 ppm (a factor of three). Therefore, it is possible to reduce the number of increments in the indirect ^{13}CO dimension by a factor of three and increase the number of scans by the same factor in order to obtain the same maximal indirect acquisition time in t_2 and t_2'. Alternatively, one may acquire additional indirect points in t_2 or t_2'.[10] For example, ^{13}CO nuclei typically have longer T_2 relaxation time in proteins relative to ^{13}CA, allowing for increased sampling of

the maximum t_2' in the SIM_2-NCOCX experiment, which would increase the resolution. These linear correction factors have previously been used in the DU-MAS technique.[10]

It should also be stated that while the first DARR mixing time is intended for only the ^{13}C spins, the ^{15}N nuclei that have been stored along the z-axis may also undergo spin diffusion. However, this will be relatively minor (< 5%) for typical mixing times of ~200 msec.[42] It is also noted that the order of the sequentially acquired experiments can be inverted to detect the NCO first (i.e., SIM_1-NCO), followed by the SIM_2-NCA experiment. In this case, the SIM_1-NCO will give the same signal/noise as the STD-NCO, while the SIM_2-NCA spectrum will have ~33% the signal/noise as the STD-NCA experiment.

Distinguishing Side Chain NH_2 Peaks in the Spectrum

In the SIM_2-NCO spectrum, it was also possible to easily distinguish the side chain NH_2 peaks from those of backbone amides in [U-^{13}C,^{15}N] samples. For the side chain Asn or Gln residues, the ^{15}N to ^{13}CA SPECIFIC-CP does not transfer amine ^{15}N magnetization to ^{13}C spins, since the covalent C_γ (Asn) or C_δ (Gln) nuclei have chemical shifts of ~175 ppm (^{13}CA offset for the experiment is ~57.5 ppm). Therefore, a relatively small loss in side chain signal (~25%) was observed in the SIM_2-NCO spectrum relative to that of the STD-NCO. The side chain amine peaks are highlighted in the SIM_2-NCO experiment in Figure 2 and displayed as 1D cross-sections in Figure 3E and F. For [U-^{13}C,^{15}N] samples, this means these peaks are the most intense in the spectrum and are easily distinguishable from those of the backbone NCO cross peaks. Since the ^{15}N amine resonances can overlap with those from the amide ^{15}N of Ser, Gly, and Thr, the intensity of the peaks can be used to easily distinguish these residue types for the purpose of spectral assignment.

Application to Selective Glycerol Labeling in Ubiquitin

A common way to improve resolution and reduce spectral congestion is the use of selective labeling schemes.[45,46] One of the preferred methods is glycerol labeling ([1,3-^{13}C] or [2-^{13}C]) that significantly reduces pairwise ^{13}C labels (i.e., few ^{13}C-^{13}C covalent bonds). This decreases resonance linewidths by removing one-bond carbon-carbon J-couplings and eliminates many of the resonances in a given spectrum.[36,37] It is also common to use glycerol or reverse labeling[47] in conjunction with double CP[48,49] or REDOR based dephasing[50-53] to assist in the assignment process.[48,49] We applied our sequential acquisition pulse sequence to ubiquitin labeled with [1,3-^{13}C] glycerol and detected SIM_1-NCA and SIM_2-NCO 2D spectra at the same time (Figure 4). Selected 1D cross sections are shown in Figure 5 for a simpler comparison. In general, we found that several of the peaks in the NCA and NCO based spectra were missing as expected from the isotopic labeling pattern (e.g., Gly resonances at 45 ppm in the SIM_1-NCA).[36,37] In fact, on average we observed that the SIM_2-NCO gave 63 ± 9% of the sensitivity compared to the STD-NCO spectrum (Figure 6). The primary advantage of our approach for partially labeled samples is to maintain no loss in sensitivity for the SIM_1-NCA dataset, while also obtaining a complementary dataset compared to that for [U-^{13}C,^{15}N] samples. In other words, the ^{15}N to ^{13}CA SPECIFIC-CP element acts as an isotope filter that can be used to assign peaks.[48] For uniformly labeled samples, the spectral information for backbone amide peaks between STD-NCO and SIM_2-NCO contains identical information, since all sites have ^{13}C labeling. However, for the [1,3-^{13}C] glycerol sample, the incorporation at the ^{13}CA depends on the residue type.[36,37] As a way to illustrate this, we plot the intensity retention as a histogram in Figure 6 comparing the uniform vs. glycerol labeling. The retention was calculated as the SIM_2-NCO peak intensity divided by the same resonance in the STD-NCO. Only resolved peaks were used in this calculation and all resonances analyzed are the same for the glycerol and uniform labeling. The wide distribution of intensity retentions compared to that obtained

for the [U-^{13}C,^{15}N] ubiquitin sample shows that the sequential acquisition approach can be used to assign resonances in a similar way as done previously.[48,54]

Discussion

Developments in magnetic resonance spectroscopy aim to improve the rate of characterizing biomolecular structure, dynamics, and imaging. We introduced a simple approach to utilizing residual or *afterglow* magnetization from the ^{15}N double CP experiment to obtain a second multidimensional dataset that can be used to assign biomolecules by SSNMR. In current practice this residual magnetization is neither refocused nor directly detected. Since one of the most important factors determining experimental length is the recycle time (time needed to obtain equilibrium), methods such as RELOAD[55] and use of paramagnetic agents[56-58] strive to reduce or eliminate the need for the long recycle delays. Our method detects two heteronuclear correlation spectra (NCA and NCO) back to back with no recycle delay between experiments. This means two datasets can be acquired for the same amount of time as the standard acquisition that gives only a single dataset. For [U-^{13}C,^{15}N] ubiquitin, we have shown that the SIM_2-NCO gives 33% of the sensitivity as the STD-NCO dataset and 50% the signal/noise as the SIM_1-NCA. This means that an additional dataset with excellent signal/noise can be obtained with no loss in sensitivity to the first dataset when compared to the standard method. Related methods have utilized multiple cross-polarization elements to improve sensitivity[59] or cross depolarization filtering techniques.[60] Note that it is possible to carry novel non-selective ^{15}N to ^{13}C double CP transfer,[26] but this compromises the sensitivity of the NCA region by ~30%.

Our sequential acquisition method is also amenable to selective glycerol or reverse labeling approaches. Since these samples have dilute ^{13}C spins, it is possible to obtain two datasets with nearly the same signal/noise without compromising the sensitivity of the spectrum acquired first. An application of our approach is the use of selectively labeled protein samples to aide in the assignment of overlapped spectra. This is important for poorly dispersed ^{15}N signals such as membrane proteins that often do not allow for robust assignments from triple resonance experiments.[52,61] While some well-ordered membrane proteins give excellent spectra,[62-64] several other membrane proteins have biologically relevant conformational disorder[65-69] that gives rise to broader spectral lines. Future developments such as TROSY based methods may aide in reducing ^{15}N line-widths that are broadened from N-H motion on the nsec to μsec timescale.[70]

In summary, the presented method uses “afterglow” ^{15}N magnetization remaining from the initial double CP step to obtain a second high quality dataset. The acquisition of these 2D or 3D datasets relies on long $T_{1\rho}$ and T_1 relaxation times that exist for ^{15}N in SSNMR.[71] Our approach is also compatible with several existing techniques, including the DU-MAS method,[10,72] paramagnetic-based sensitivity enhancement methods,[56-58] dynamic nuclear polarization experiments,[73] applications utilizing time-resolved MAS techniques,[74-76] and oriented SSNMR. This method requires no additional SSNMR hardware and will result in no loss in sensitivity for the first dataset. The second dataset is *free* and can be detected with good sensitivity for biomolecular assignments in MAS SSNMR spectroscopy.

Acknowledgments

The authors thank Prof. Alexej Jerschow for a careful reading of the manuscript. This work was supported by NIH grant 5K22AI083745 and start up funds from New York University.

References

(1). McDermott AE. Curr Opin Struct Biol. 2004; 14:554–561. [PubMed: 15465315]

(2). Opella SJ, Marassi FM. Chem Rev. 2004; 104:3587–3606. [PubMed: 15303829]
(3). Hong M. J Phys Chem B. 2007; 111:10340–10351. [PubMed: 17685648]
(4). Tycko R. Ann Rev Phys Chem. 2011; 62:279–299. [PubMed: 21219138]
(5). Baldus M. Curr Opin Struct Biol. 2006; 16:618–623. [PubMed: 16942870]
(6). Naito A. Solid State Nucl Magn Reson. 2009; 36:67–76. [PubMed: 19647984]
(7). Wylie BJ, Rienstra CM. J Chem Phys. 2008; 128:052207. [PubMed: 18266412]
(8). Herbst C, Riedel K, Ihle Y, Leppert J, Ohlenschlager O, Gorlach M, Ramachandran R. J Biomol NMR. 2008; 41:121–125. [PubMed: 18516685]
(9). Kupce E, Kay LE, Freeman R. J Am Chem Soc. 2010; 132:18008–18011. [PubMed: 21126087]
(10). Gopinath T, Veglia G. Angewandte Chemie (International ed.in English). 2012
(11). Kupce E, Freeman R, John BK. J Am Chem Soc. 2006; 128:9606–9607. [PubMed: 16866495]
(12). Pines A, Gibby MG, Waugh JS. J Chem Phys. 1973; 59:569–590.
(13). Lurie FM, Slichter CP. Phys Rev Lett. 1963; 10:403.
(14). Hartmann SR, Hahn EL. Phys Rev. 1962; 128:2042.
(15). Schaefer J, Stejskal EO. J Am Chem Soc. 1976; 98:1031–1032.
(16). Levitt MH, Suter D, Ernst RR. J Chem Phys. 1986; 84:4243–4255.
(17). Fukuchi M, Ramamoorthy A, Takegoshi K. J Magn Reson. 2009; 196:105–109. [PubMed: 19022690]
(18). Kolodziejski W, Klinowski J. Chem Rev. 2002; 102:613–628. [PubMed: 11890752]
(19). Hediger S, Meier BH, Ernst RR. Chem Phys Lett. 1993; 213:627–635.
(20). Hediger S, Meier BH, Ernst RR. Chem Phys Lett. 1995; 240:449–456.
(21). Nevzorov AA. J Magn Reson. 2011; 209:161–166. [PubMed: 21296016]
(22). Baldus M, Geurts DG, Hediger S, Meier BH. J Magn Reson Ser A. 1996; 118:140–144.
(23). Baldus M, Petkova AT, Herzfeld JH, Griffin RG. Mol Phys. 1998; 95:1197–1207.
(24). Metz G, Wu XL, Smith SO. J Magn Reson Ser A. 1994; 110:219–227.
(25). Schaefer J, McKay RA, Stejskal EO. J Magn Reson. 1979; 34:443–447.
(26). Zhang Z, Miao Y, Liu X, Yang J, Li C, Deng F, Fu R. J Magn Reson. 2012; 217:92–99. [PubMed: 22445831]
(27). Nielsen AB, Straaso LA, Nieuwkoop AJ, Rienstra CM, Bjerring M, Nielsen NC. J Phys Chem Lett. 2010; 1:1952–1956. [PubMed: 20689682]
(28). Brinkmann A, Levitt MH. J Chem Phys. 2001; 115:357–384.
(29). Lee YK, Kurur ND, Helmle M, Johannessen OG, Nielsen NC, Levitt MH. Chem Phys Lett. 1995; 242:304–309.
(30). Bjerring M, Nielsen NC. Chem Phys Lett. 2003; 370:496–503.
(31). Kehlet C, Bjerring M, Sivertsen AC, Kristensen T, Enghild JJ, Glaser S, Khaneja N, Nielsen NC. J Magn Reson. 2007; 188:216–230. [PubMed: 17681479]
(32). Kehlet CT, Sivertsen AC, Bjerring M, Reiss TO, Khaneja N, Glaser SJ, Nielsen NC. J Am Chem Soc. 2004; 126:10202–10203. [PubMed: 15315406]
(33). Gopinath T, Veglia G. J Am Chem Soc. 2009; 131:5754–5756. [PubMed: 19351170]
(34). Gopinath T, Verardi R, Traaseth NJ, Veglia G. J Phys Chem B. 2010; 114:5089–5095. [PubMed: 20349983]
(35). Lazar GA, Desjarlais JR, Handel TM. Protein Sci. 1997; 6:1167–1178. [PubMed: 9194177]
(36). Castellani F, van Rossum B, Diehl A, Schubert M, Rehbein K, Oschkinat H. Nature. 2002; 420:98–102. [PubMed: 12422222]
(37). LeMaster DM, Kushlan DM. J Am Chem Soc. 1996; 118:9255–9264.
(38). Igumenova TI, Wand AJ, McDermott AE. J Am Chem Soc. 2004; 126:5323–5331. [PubMed: 15099118]
(39). Franks WT, Kloepper KD, Wylie BJ, Rienstra CM. J Biomolec NMR. 2007; 39:107–131.
(40). Takegoshi K, Nakamura S, Terao T. Chem Phys Lett. 2001; 344:631–637.

(41). Loening NM, Bjerring M, Nielsen NC, Oschkinat H. J Magn Reson. 2012; 214:81–90. [PubMed: 22116035]

(42). Seidel K, Etzkorn M, Heise H, Becker S, Baldus M. Chembiochem. 2005; 6:1638–1647. [PubMed: 16094694]

(43). Schubert M, Manolikas T, Rogowski M, Meier BH. J Biomolec NMR. 2006; 35:167–173.

(44). Igumenova TI, McDermott AE, Zilm KW, Martin RW, Paulson EK, Wand AJ. J Am Chem Soc. 2004; 126:6720–6727. [PubMed: 15161300]

(45). Hong M, Jakes K. J Biomolec NMR. 1999; 14:71–74.

(46). Lian LY, Middleton DA. Prog Nucl Magn Reson Spectrosc. 2001; 39:171–190.

(47). Vuister GW, Kim SJ, Wu C, Bax A. J Am Chem Soc. 1994; 116:9206–9210.

(48). Higman VA, Flinders J, Hiller M, Jehle S, Markovic S, Fiedler S, van Rossum BJ, Oschkinat H. J Biomolec NMR. 2009; 44:245–260.

(49). Shi L, Ahmed MA, Zhang W, Whited G, Brown LS, Ladizhansky V. J Mol Biol. 2009; 386:1078–1093. [PubMed: 19244620]

(50). Yang J, Tasayco ML, Polenova T. J Am Chem Soc. 2008; 130:5798–5807. [PubMed: 18393505]

(51). Li S, Su Y, Luo W, Hong M. J Phys Chem B. 2010; 114:4063–4069. [PubMed: 20199036]

(52). Traaseth NJ, Veglia G. J Magn Reson. 2011; 211:18–24. [PubMed: 21482162]

(53). Yang J, Parkanzky PD, Bodner ML, Duskin CA, Weliky DP. J Magn Reson. 2002; 159:101–110. [PubMed: 12482688]

(54). Sperling LJ, Berthold DA, Jeisy Sasser TL, Scott V, Rienstra CM. J Mol Biol. 2010; 399:268–282. [PubMed: 20394752]

(55). Lopez JJ, Kaiser C, Asami S, Glaubitz C. J Am Chem Soc. 2009; 131:15970–15971. [PubMed: 19886687]

(56). Wickramasinghe NP, Shaibat M, Ishii Y. J Am Chem Soc. 2005; 127:5796–5797. [PubMed: 15839671]

(57). Nadaud PS, Helmus JJ, Kall SL, Jaroniec CP. J Am Chem Soc. 2009; 131:8108–8120. [PubMed: 19445506]

(58). Yamamoto K, Xu J, Kawulka KE, Vederas JC, Ramamoorthy A. J Am Chem Soc. 2010; 132:6929–6931. [PubMed: 20433169]

(59). Tang W, Nevzorov AA. J Magn Reson. 2011; 212:245–248. [PubMed: 21784682]

(60). Wu XL, Zhang SM, Wu XW. Phys Rev B. 1988; 37:9827–9829.

(61). Agarwal V, Fink U, Schuldiner S, Reif B. Biochim Biophys Acta. 2007; 1768:3036–3043. [PubMed: 17976529]

(62). Ward ME, Shi L, Lake E, Krishnamurthy S, Hutchins H, Brown LS, Ladizhansky V. J Am Chem Soc. 2011; 133:17434–17443. [PubMed: 21919530]

(63). Li Y, Berthold DA, Frericks HL, Gennis RB, Rienstra CM. Chembiochem. 2007; 8:434–442. [PubMed: 17285659]

(64). Shi L, Kawamura I, Jung KH, Brown LS, Ladizhansky V. Angew Chem Int Ed Engl. 2011; 50:1302–1305. [PubMed: 21290498]

(65). Mittag T, Kay LE, Forman Kay JD. J Molec Recog. 2010; 23:105–116.

(66). Gustavsson M, Traaseth NJ, Karim CB, Lockamy EL, Thomas DD, Veglia G. J Mol Biol. 2011; 408:755–765. [PubMed: 21419777]

(67). Gustavsson M, Traaseth NJ, Veglia G. Biochim Biophys Acta. 2012; 1818:146–153. [PubMed: 21839724]

(68). Hong M, Zhang Y, Hu F. Annu Rev Phys Chem. 2011

(69). Su Y, Hong M. J Phys Chem B. 2011; 115:10758–10767. [PubMed: 21806038]

(70). Chevelkov V, Faelber K, Schrey A, Rehbein K, Diehl A, Reif B. J Am Chem Soc. 2007; 129:10195–10200. [PubMed: 17663552]

(71). Schanda P, Meier BH, Ernst M. J Am Chem Soc. 2010; 132:15957–15967. [PubMed: 20977205]

(72). Gopinath T, Veglia G. J Magn Reson. 2012 in press.

(73). Maly T, Debelouchina GT, Bajaj VS, Hu KN, Joo CG, Mak Jurkauskas ML, Sirigiri JR, van der Wel PC, Herzfeld J, Temkin RJ. J Chem Phys. 2008; 128:052211. [PubMed: 18266416]

(74). Evans JNS, Appleyard RJ, Shuttleworth WA. J Am Chem Soc. 1993; 115:1588–1590.
(75). Hu KN, Yau WM, Tycko R. J Am Chem Soc. 2010; 132:24–25. [PubMed: 20000466]
(76). Comellas G, Lemkau LR, Zhou DH, George JM, Rienstra CM. J Am Chem Soc. 2012; 134:5090–5099. [PubMed: 22352310]

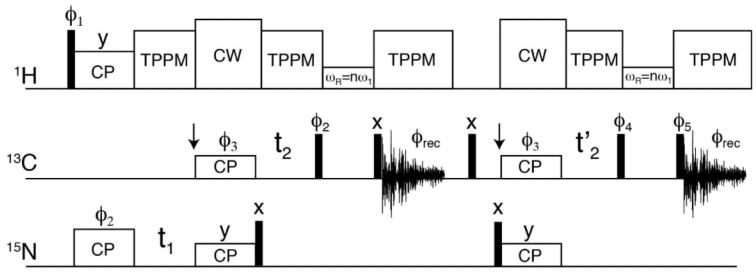

Figure 1.

Pulse sequence with two acquisitions for simultaneous detection of 2D SIM_1-NCA and SIM_2-NCO or 3D SIM_1-NCACX and SIM_2-NCOCX spectra. The former are achieved by setting the DARR mixing time to zero. The DARR mixing can be replaced with a double quantum transfer for improved single bond transfers. The narrow rectangles correspond to 90° pulses. Phase are: ϕ_1=(x,−x), ϕ_2=(y), ϕ_3=(x,x,y,y), ϕ_4=(−y,−y,−x,−x), ϕ_5=(y,y,−x,−x), and ϕ_{rec}=(x,−x,−y,y). To obtain phase-sensitive data in t_1 and t_2, ϕ_2 and ϕ_3 were phase-shifted by 90°, respectively. After the first FID acquisition, a 5 msec time was allowed to dephase residual ^{13}C magnetization; during this time a $90_x°$ pulse was applied ^{13}C.

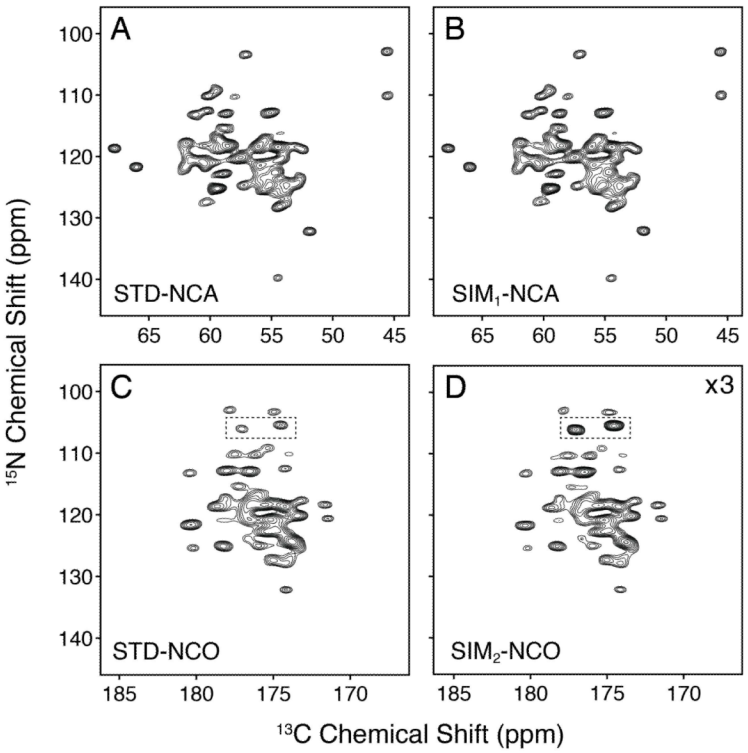

Figure 2.

Comparison of the standard vs. sequentially acquired datasets on [U-^{13}C,^{15}N] ubiquitin. The STD-NCA and STD-NCO datasets (A and C) used identical experimental parameters as the sequentially acquired ones (B and D). The spectra in panels A and B are each plotted starting at a contour level of 18.75. This is a factor of 1.5 higher than the SIM$_2$-NCO dataset (panel D; first contour: 12.5). The SIM$_2$-NCO spectrum (panel C) is plotted at 3 times the signal level compared to the STD-NCO (first contour: 37.5), which accounts for the signal loss in the SIM$_2$-NCO from the SPECIFIC-CP transfer to ^{13}CA. For the listed contour levels, the standard deviation of the noise is 1.0. The peaks in the dotted rectangles indicate side chain residues that have 75% intensity retention. The 2D datasets for the STD-NCA and STD-NCO together required 2 times longer acquisition than that for the SIM$_1$-NCA and SIM$_2$-NCO.

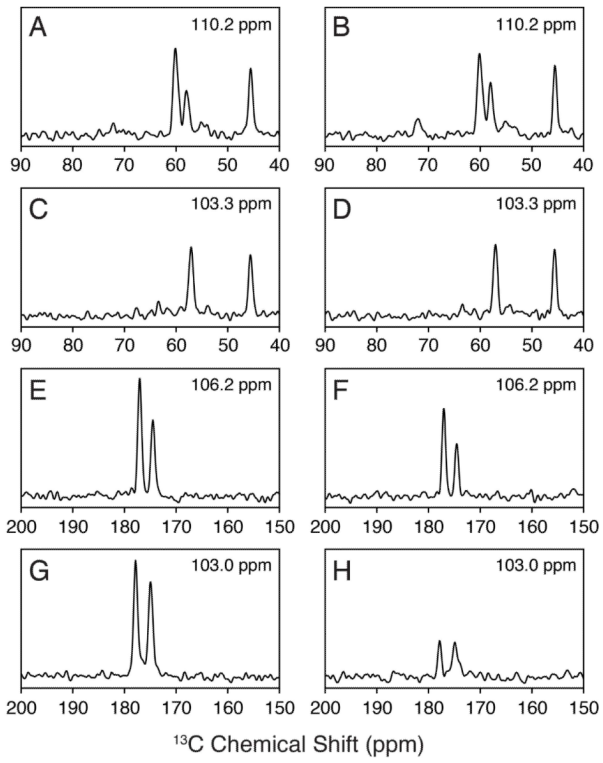

Figure 3.

1D cross-sections of the 2D spectra shown in Figure 2 for [U-^{13}C,^{15}N] ubiquitin. The ^{15}N frequencies are given in each panel. The STD-NCA 1D cross sections (A, C) can be directly compared with those of the SIM1-NCA dataset (B, D). As expected these peak intensities are identical. The STD-NCO cross sections (E, G) are directly compared to those of the SIM2-NCO (F, H). The noise level is the same in all 1D spectra. The spectra in panels E and F correspond to side chain $^{15}NH_2$ resonances.

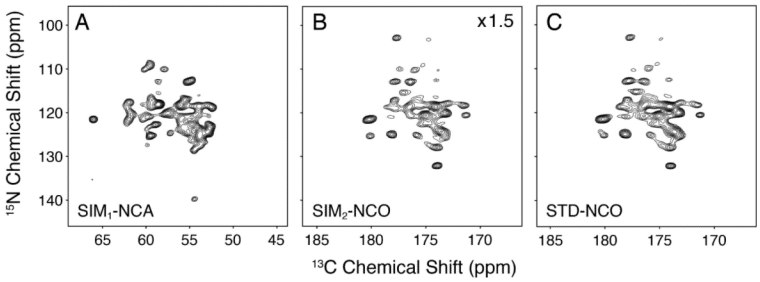

Figure 4.

Comparison of the standard vs. sequentially acquired datasets on [1,3-^{13}C] glycerol labeled ubiquitin. The STD-NCA (not shown) is identical to that of the SIM$_1$-NCA (panel A). All comparable experimental parameters were the same between the STD-NCO (panel C) and the SIM$_2$-NCO (panel B). The sequentially acquired datasets in panels A and B are plotted at the same noise level (first contour: 11.0). The SIM$_2$-NCO spectrum (panel B) is plotted at 1.5 times the signal level compared to the STD-NCO (panel C; first contour: 16.5); this accounts for the average signal loss in the SIM$_2$-NCO due to the SPECIFIC-CP transfer to ^{13}CA. For the listed contour levels, the standard deviation of the noise is 1.0.

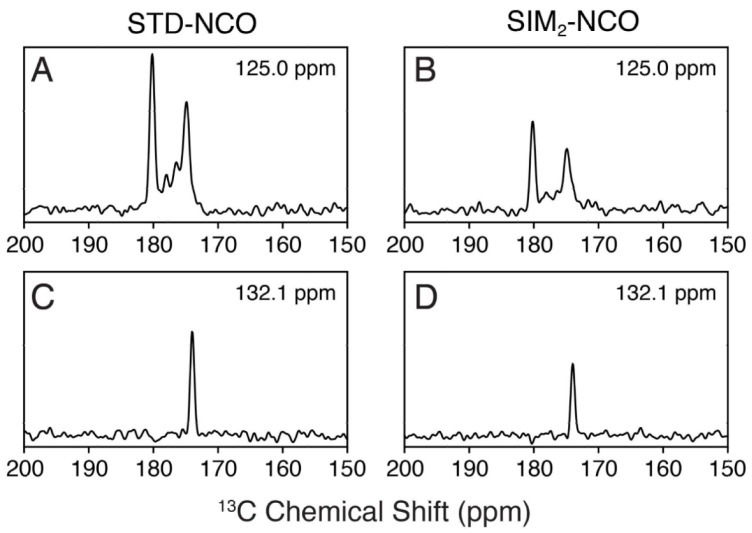

Figure 5.

1D cross sections of the 2D spectra shown in Figure 4 for the [1,3-^{13}C] glycerol labeled ubiquitin sample. The ^{15}N frequencies indicated in each panel are directly comparable for the STD-NCO (A, C) and SIM_2-NCO spectra (B, D). The noise level is the same for the four 1D cross-sections.

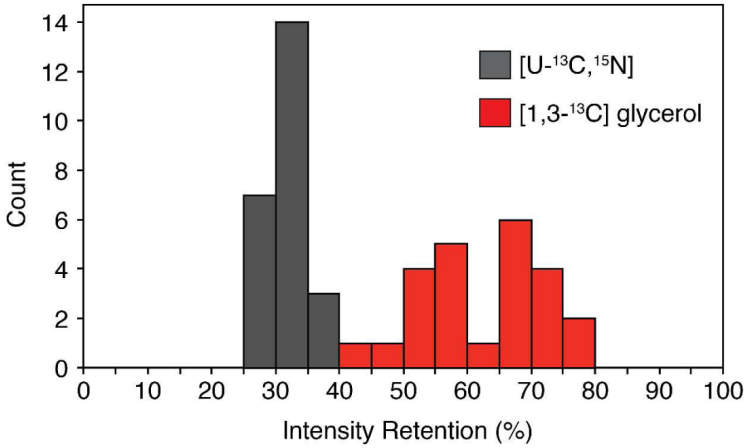

Figure 6.

Histogram of intensity retention for the [1,3-^{13}C] glycerol vs. [U-^{13}C,^{15}N] labeling ubiquitin samples. The intensity retention is calculated by dividing the intensity of the resolved peak in the 2D SIM_2-NCO spectrum by the corresponding resonance in the 2D STD-NCO. In total 24 resolved peaks from the 2D spectra from Figures 2 and 4 were used for this analysis. The average ± standard deviation for the two samples are: [U-^{13}C,^{15}N] = 32 ± 3%, [1,3-^{13}C] glycerol = 63 ± 9%.